https://doi.org/10.5194/os-2019-86
Preprint. Discussion started: 19 August 2019

Ocean Science
Discussions
Open Access
EGU

A Comparison of Ocean Model Results with Satellite Observations during the Development of the strong 1997-98 El Niño

David J. Webb, Andrew C. Coward, and Helen M. Snaith
National Oceanography Centre, Southampton SO14 3ZH, U.K.
Correspondence: D.J.Webb (djw@noc.ac.uk)

Abstract. Satellite data from the equatorial Pacific is compared with results from a high resolution ocean model during a period including the strong El Niño of 1997-98. The results show that the ocean model realistically captures the changes in sea surface temperature and the propagation of the annual Rossby wave although it may overestimate the reduced energy of tropical instability waves during development of an El Niño. The results provide additional confidence in the oceanic mechanisms which model analysis implicated as being responsible for the development of both the 1982-83 and the 1997-98 El Niños.

1 Introduction

Wyrtki (1973, 1974) analysed sea level time series at Pacific islands and showed that there was a correlation between the occurance of strong El Niños and an increase in the sea level difference across the North Equatorial Counter Current. This current lies near 5°N and carries near surface ocean water from the warm western equatorial Pacific into the eastern Pacific, north of the Galapagos.

The increased sea level difference implies an increased pressure difference within the ocean and, as with pressure differences in the atmosphere, this in turn implies an increase in the current. Wyrtki surmised that the increased current would transport more warm surface water from the western to the eastern Pacific. Here it would trigger strong convection in the atmosphere and so trigger an El Niño.

Unfortunately the work was published at a time when analytic and numerical models of the equatorial ocean were leading researchers in another direction. Thus Anderson and Rowlands (1976) and McCreary (1978) both showed that Kelvin waves caused upwelling on Central America, the implication being that this could cause warming of the surface layer sufficient to generate an El Niño (Gill, 1982).

This led to an emphasis on the potential role of equatorial Kelvin waves in triggering El Niños. Indeed Wyrtki's own theory of the El Niño (Wyrtki, 1975) states that "the accumulated water flows eastward, probably in the form of an internal equatorial Kelvin wave" and "This wave leads to an accumulation of warm water off Ecuador and Peru".

However although equatorial Kelvin waves can readily transport energy and momentum, wave motions are very inefficient at transporting mass and related properties such as salinity and heat. Kelvin waves might trigger another process which heats the eastern Pacific but although internal Kelvin waves can warm the deep ocean through downward advection, there is no way in which the reverse process can warm the surface layer.

https://doi.org/10.5194/os-2019-86
Preprint. Discussion started: 19 August 2019

This problem of the heat transport during an El Niño, was investigated by Webb (2018) using archived data from a 1/12°global ocean model. The study concentrated on the strong El Niños of 1982-83 and 1997-97 and found that equatorial Kelvin waves had no significant effect on the surface temperature of the eastern Pacific.

Instead the model results showed that both the temperature and volume of water carried by the North Equatorial Counter Current (NECC) increased during the period that the El Niños were growing.

This resulted in water reaching the eastern Pacific which being above 28°C, was warm enough to trigger deep atmospheric convection. This occurred near the latitude of the Inter Tropical Convergence Zone (ITCZ), the band where the where the atmosphere is more unstable than normal. As a result it was concluded that it was this water which triggered the strong El Niños.

1.1 Mechanisms

The model results also indicated that three physical mechanisms were involved. The first was an increased strength of the NECC due to the annual Rossby wave which, in the western Pacific, was particularly strong in mid-1982 and mid-1997. The Rossby wave lowers sea level near 6°N, increasing the pressure difference across the NECC and also moving the current towards the Equator, increasing its transport. The result supports Wyrtki's observations (Wyrtki, 1973, 1974) discussed above.

The second mechanism that acted during the development of the El Niños involved an increase in the core temperature of the NECC resulting from a reduction in the strength of tropical instability waves (or eddies). In a normal year the eddies extract warm water from the core of the NECC and replace it with cooler water, so reducing the temperature of the current.

However as the El Niños develop, a region of deep convection develops with low winds along the Equator. The low winds reduce the strength of the Equatorial Current and as a consequence the magnitude of the instability waves is also reduced. With mixing reduced, the NECC carries warm water further east, triggering a new region of deep atmospheric convection and so repeating the process.

Finally the model confirmed a third mechanism, originally proposed by Kug et al. (2009), where the region of highest sea level on the equator, moves from the western Pacific into the central Pacific. This increases the pressure difference across the NECC in the central Pacific again increasing its transport of warm surface water towards the eastern Pacific.

1.2 Comparison with Observations

But these are just model results and, given the widespread acceptance of the Kelvin wave ideas[1], both the results and the mechanisms proposed need to be carefully checked against observations.

To a certain extent this has been done, Webb (2016) investigating surface temperatures in the five Pacific Niño regions and showing good agreement between the model and observations. That study also investigated whether the changes occurring during an El Niño were due to advection, other model processes or feedback between the model and the atmospheric forcing. The results indicated that any feedback was cooling the ocean surface and that warming during the development of the strong El Niños was due primarily to advection.

[1] See for example Wikipedia "Equatorial wave" (version of 11 March 2019).

https://doi.org/10.5194/os-2019-86
Preprint. Discussion started: 19 August 2019

Ocean Science
Discussions
Open Access
EGU

In the present study further checks of the model are carried out using satellite data from the 1995-2000 to check the model sea surface temperature (SST) and sea surface height (SSH) fields in regions most affected by the three mechanisms discussed above.

The SST values are important because, as discussed by Evans and Webster (2014), it is only when SST rises above 28°C, that deep atmospheric convection can occur. SSH is important because, in the model, the annual Rossby wave and tropical instability waves show up clearly in sea surface height signal. As a result, satellite based radar altimeters, which measure sea level to within a few centimetres, provide a useful check on both the Rossby wave and the tropical instability waves as seen in the model.

There were no altimeter measurements of SSH during the 1982-83 period but by 1997-98, both the Topex-Poseidon and ERS-2 satellite altimeters were operating. This paper thus concentrates on the later period.

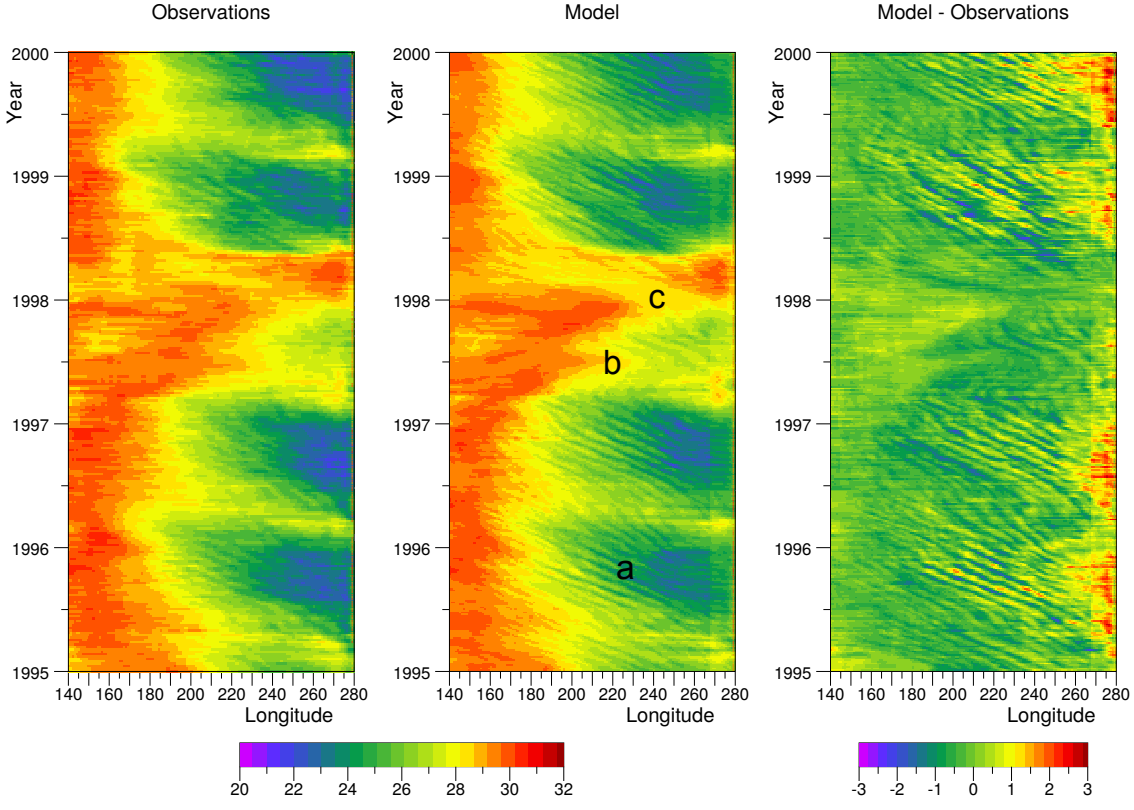

Figure 1. Observed and model sea surface temperatures and their difference, averaged between 5°S and 5°N, for the equatorial Pacific between 140°E and 280°E (80°W). Showing (a) Tropical Instability Waves, strongest in second half of non-El Niño years, (b) initial mid-ocean El Niño, discussed in Webb (2018), (c) strong El Niño, starting in the west around mid-year and arriving in the east around new year. Temperature units are degrees C.

https://doi.org/10.5194/os-2019-86
Preprint. Discussion started: 19 August 2019

Section 2 discusses the model and satellite data and the processing used to generate the gridded data sets used here. Section 3 is concerned with the sea surface temperature signal. Section 4 then compares the altimeter and model sea levels across the Pacific at 6°N, a key latitude for the propagation of the annual Rossby wave, and at the Equator. At 6°N the tropical instability waves show up as propagating waves allowing, in Section 5, a comparison of the strength of the waves in the model and observations.

Although the overall qualitative agreement between model and observations is good, in the periods when the instability waves are weakest, the variance in the model data is much smaller than in the observations - as though the model is too quiet. The final section reviews the results and discusses how they support, or fail to support, the proposed mechanisms controlling the growth of a strong El Niño.

2 Data Sources and Processing

The model data used in this paper is from the five day average datasets generated during run 6 of the Nemo 1/12°model. This is the same data as used for Webb (2016) and Webb (2018), where detailed information on the model, the model run and the archive datasets can be found. The model data is on a 1/12 degree grid but, for the comparisons reported here, sea surface values were averaged onto the same grid as used for the processed satellite data.

The processed sea surface temperature used in this paper is the weekly averaged version of the Reynolds Optimally Interpolated satellite data (Reynolds and Stokes, 1981). The analysis scheme, described in Reynolds et al. (2002), combines data from separate satellites and corrects for the effects of clouds and other errors in the measurements. The data is provided in the form of averages over one-degree cells.

The processed satellite altimeter data is the Copernicus DUACS DT2014 gridded absolute dynamic topography dataset Pujol et al. (2016); Taburet and Team. For the period studied here this combines the altimeter measurements of the ERS-2 and Topex/Poseidon satellites, correcting for errors and using optimal interpolation to generate data on a 1/4-degree grid at daily intervals.

For the analysis reported here the satellite altimeter data was averaged over the same five day periods as used by the ocean model.

There are some reservations aboout the altimeter which need to be kept in mind. Pujol et al. (2016) refer to error variances of up to 32.5 cm^2 in energetic regions of ocean and Taburet and Team state that two satellites are the "minimum for offline applications". They also show that the effective spatial resolution of the gridded data may be 200 km and more in the equatorial regions discussed here.

3 Comparison of Sea Surface Temperatures

Figure 1 compares the sea surface temperature (SST) averaged between 5°S and 5°N for the period 1995 to 2000. Both the model and observations show the 1997-98 El Niño developing in two stages, an initial advance of warm water towards the

https://doi.org/10.5194/os-2019-86
Preprint. Discussion started: 19 August 2019

Ocean Science
Discussions
Open Access
EGU

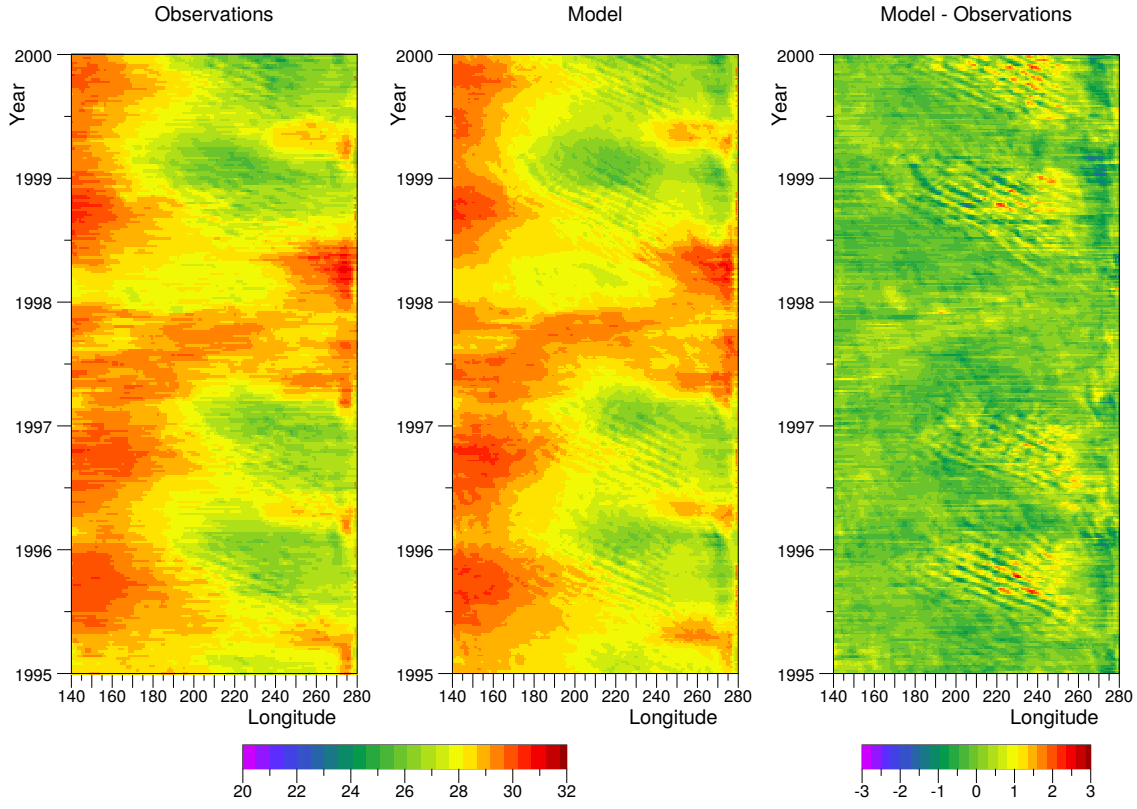

Figure 2. Observed and model sea surface temperatures and their difference, averaged between 3°N and 9°N, for the equatorial Pacific between 140°E and 280°E (80°W). Units are degrees C.

central Equatorial Pacific between March and June 1997, followed by the main El Niño advance which starts during late (northern) summer and reaches the eastern boundary of the Pacific in early 1998.

As discussed in Webb (2018) the first advance may have been triggered by winds crossing the Equator north of New Guinea. The following main advance is then consistent with the development of an enhanced North Equatorial Counter Current (NECC) arising from a stronger than normal annual Rossby wave.

The results show that the observations and model are generally in good agreement in both the magnitude and the timing, not only of the El Niño but also of the many other features seen in the figures. For the El Niño, the main discrepancy occurs in the central Pacific where the difference figure shows that the model is up to one degree warmer than the observations.

The model is also warmer than observations in the eastern Pacific where there appears to be a jump in model temperatures east of the Galapagos Islands at 270°E. This may be a problem due to the model topography, the relatively coarse model representation of the islands partly blocking both the Equatorial Current and Equatorial Undercurrent.

https://doi.org/10.5194/os-2019-86
Preprint. Discussion started: 19 August 2019

Ocean Science
Discussions
Open Access
EGU

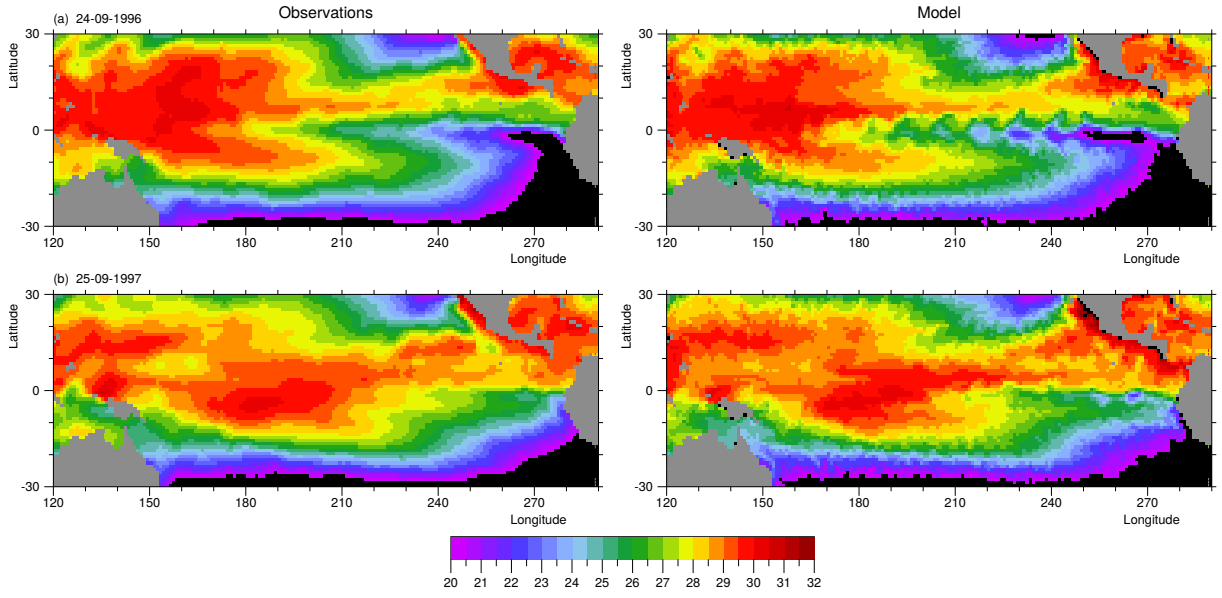

Figure 3. Observed and Model Sea Surface Temperatures in (a) late September 1996 and (b) late September 1997. Units are degrees C. For these figures the model data has been averaged onto the same one-degree grid as used for the satellite based dataset.

In addition the figures show that, outside the El Niño years, the central Pacific temperature anomalies due to tropical instability waves appear larger in the model data set than in the observations. However after allowing for this, there is agreement with the model in both the east-west wavelength of the waves and the variations in the speed as they propagate westwards. The differences in the amplitudes may be due to model errors but they could also be due to smoothing of the observations by the optimal interpolation process.

The waves are emphasised in the difference plot, as would be expected for chaotic events. In this respect the lack of any short wavelength features in the difference plot during the second half of 1997, when the El Niño was growing, is significant.

The mechanisms proposed by Webb (2018) mainly involved the transport of heat by the NECC. Unfortunately the current lies partly outside the equatorial band of Fig 1, so as a check Fig. 2 shows a similar comparison for the latitude range 3°N and 9°N. This includes most of the NECC and is centred on the 6°N latitude discussed later. It also covers most of the latitude range of the ITCZ where the atmosphere appears to be most unstable.

The figures again illustrate good agreement between model and observations and, as discussed below, show that during the development of the El Niño, when the central Pacific warms, there is a cooling of the western Pacific at these latitudes.

The tropical instability waves between 3°N an 9°N are slightly weaker than those of Fig. 1, but in both cases the difference plot shows that during the El Niño they all but disappear in the central Pacific.

https://doi.org/10.5194/os-2019-86
Preprint. Discussion started: 19 August 2019

Ocean Science
Discussions
Open Access
EGU

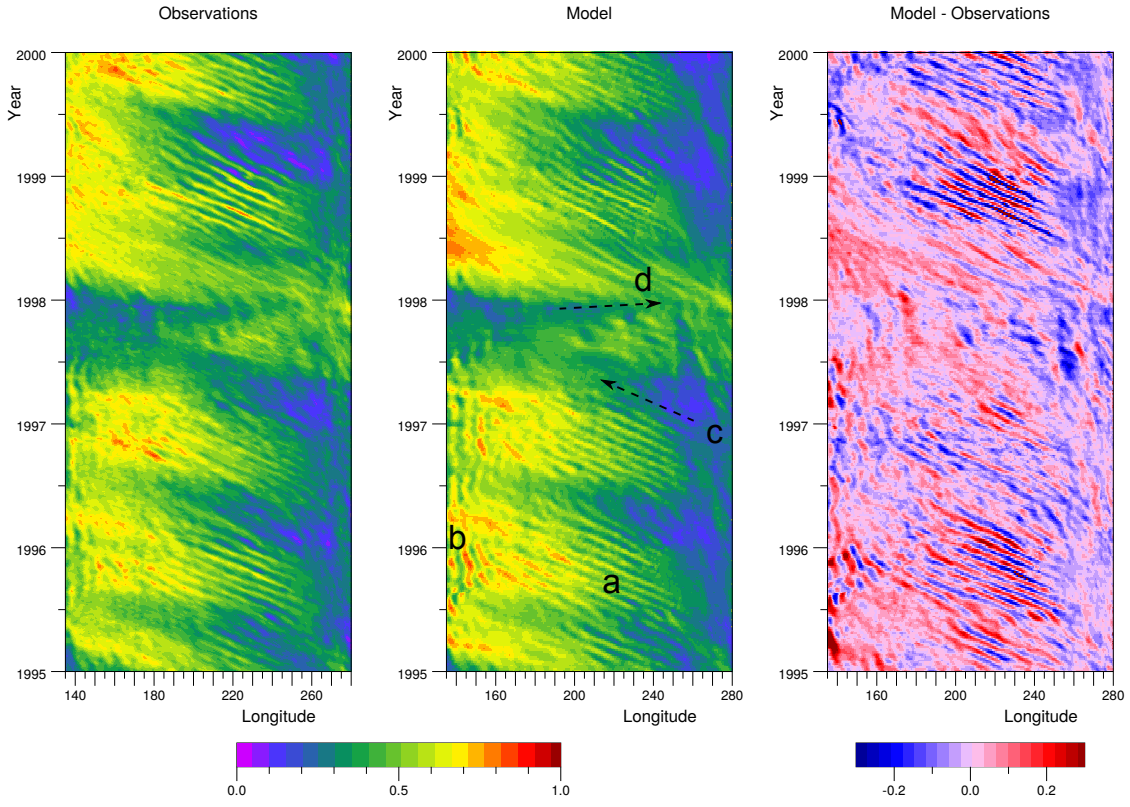

Figure 4. Observed and model sea surface height and their difference in the Pacific at latitude of 6°N between 135°E and 280°E (80°W). Showing (a) westward propagating tropical instability waves or eddies, (b) quasi-steady meanders near the start of the NECC, (c) westward propagating annual Rossby wave, (d) eastward propagating Kelvin wave. Units are metres.

3.1 Surface Temperature Maps

The El Niño is usually characterised in terms of the average sea surface temperatures between 5°N and 5°S. However the model results reported by Webb (2018) indicate that the most significant changes occur further north.

Here, during the development of an El Niño, the North Equatorial Counter Current can transport significant amounts of warm water into the eastern Pacific near the latitude of the atmospheric Inter-Tropical Convergence Zone (ITCZ). There the warm water can trigger enhanced deep atmospheric convection and thus be the cause of a strong atmospheric El Niño.

Figure 3 compares the observed and model fields of SST during late September in 1996, a normal year, and in 1997, during the development of the 1997-98 El Niño. Late September is of interest because, as discussed in Webb (2018), during the development of a strong El Niño it shows two important features.

https://doi.org/10.5194/os-2019-86
Preprint. Discussion started: 19 August 2019

The first, the result of enhanced transport by the NECC is the region of enhanced SST north of the Equator in the eastern Pacific. The second is the region of high SSTs that develops in the central Pacific. As is discussed later, the latter also shows a maximum in sea level, possibly because it lies between regions of easterly and westerly winds acting along the Equator.

The results for September 1996, show generally good agreement. The most obvious difference occurs along the Equator in the central and eastern Pacific where the the Tropical Instability waves are much more pronounced in the model plot than in the observations. Plots of individual satellite SST measurements, for example Wentz et al. (2000), usually show much stronger instability waves, so it is possible that the Reynolds SST processing has smoothed out these features.

There is also good agreement in September 1997. Both the observations and the model show a region of high temperatures at the latitude of the NECC which extends from the central Pacific into the eastern Pacific. The model results showed that this water had been advected from the west. In support of this, both figures show a region of reduced SSTs between 150°E and 170°E at the latitudes of the NECC.

Both observations and model also show the eastward shift in the region of highest SSTs along the Equator. This shift also affects temperatures south of the Equator as far as 10°S.

4 Sea Levels along 6°N and the Equator

Webb (2018) found that the increased strength of the NECC during the growth of an El Nino was in part associated with an increased sea level difference between the Equator and 6°N. It is thus of interest to see how the observations and model compare at both these latitudes.

Figure 4 compares the observed and model sea levels at 6°N (i.e. the gridded data averaged between 5.75°N and 6.25°N). Between 1995 and 1997 both behave in a similar manner, showing a similar mean east-west slope, an annual signal and small scale structures. Between 160°E and 250°E these are due to westward propagating tropical instability waves. West of 160°E they are due to the, almost steady, north-south meanders generated near the start of the NECC.

The years 1995 and 1996 also show the annual Rossby wave propagating westwards in both observations and model. In mid-1997, they both show the larger than normal drop in sea level that occurs between 160°E and 180°E. In Webb (2018) this was found to be connected with an increase in the strength of the NECC, such that it carried warm surface water further east than was normal.

In Fig. 4, as the Rossby wave reaches the western boundary near the end of 1997, both the model and observations show a drop in sea level that propagates eastwards along the Equator. This appears an equatorial Kelvin wave and marks the end of the El Niño growth phase.

Early 1998 sees the development of higher than normal sea levels in the west, in both model and observations. The standing waves due to the NECC disappear and initially so do the tropical instability waves. These reappear strongly during the second half of the year after which the ocean appears to return to its normal state.

The comparison between observations of SSH and the model results at the Equator is shown in Fig. 5. The agreement is good, both in the large scale structure and the timing of individual Kelvin waves seen to propagate eastwards across the Equatorial

https://doi.org/10.5194/os-2019-86
Preprint. Discussion started: 19 August 2019

Ocean Science
Discussions
Open Access
EGU

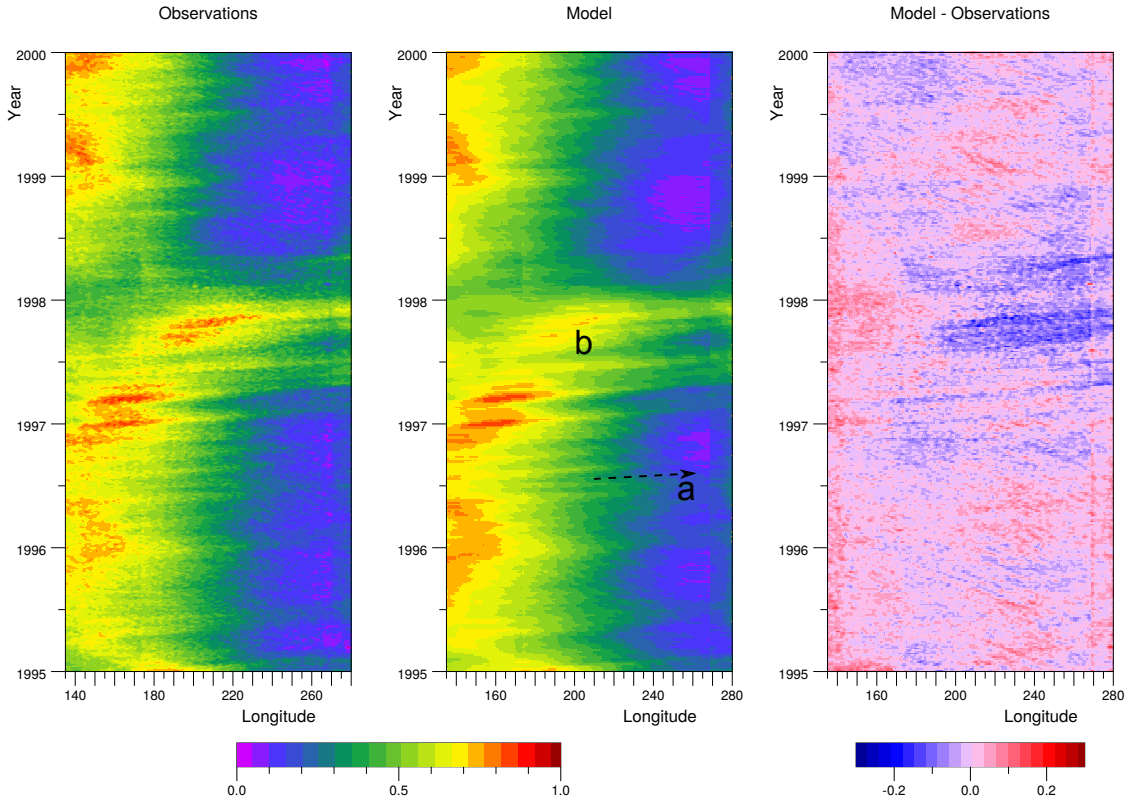

Figure 5. Observed and model sea surface height and their difference in the Pacific on the Equator between 135°E and 280°E (80°W). Showing (a) eastward propagating Kelvin waves, (b) sea level high moving to the central Pacific. Units are metres.

Ocean. Although the timing of these events seems very good, they will be a direct response to the wind forcing and so the agreement is really a measure of the quality of the wind forcing used to drive the model.

Possibly of more importance is the close agreement in the strength and position of the region of maximum sea level which, during 1997, moves from the western boundary into the centre of the Pacific. During the second and third quarters of 1997 this will have increased the sea level difference in the western Pacific between the equator and 6°N. As a result it will have been partly responsible for the enhanced strength of the NECC.

5 Mixing by Tropical Instability Waves

Webb (2018) found from the model results that the transport of warm-water by the NECC during an El Niño was also increased as a result of reduced mixing by tropical instability waves. In the paper the magnitude of the mixing was estimated by calculating the smoothed variance of the northward component of velocity in the top 300 m of the ocean at 6°N.

https://doi.org/10.5194/os-2019-86
Preprint. Discussion started: 19 August 2019


Ocean Science
Discussions
Open Access
EGU

Averages over the top few hundred metres are not available from the satellite data discussed here, but the geostrophic component of the surface velocity field can be calculated from the sea surface height. If v is the northward component of geostrophic current at the ocean surface, then,

$$v = (g/f)\,\partial h/\partial x, \tag{1}$$

where g is gravity, f the Coriolis term, h the sea surface height and x the eastwards co-ordinate.

Let $\bar{v}$, be the smoothed value, produced by averaging over a range of longitudes and let v_{rms}, be the smoothed r.m.s. variance defined in a similar way. Then,

$$\begin{aligned} \bar{v} &= H(v), \\ v_{rms} &= H(|(v-\bar{v})|). \end{aligned} \tag{2}$$

where $H()$ is a smoothing filter. For the results presented here H is a Hann filter with a width of 20°of longitude.

The results at 6°N, calculated using the above scheme, for both the satellite observations and the model are shown in Fig. 6.

In 1995 both figures show maximum variance in the eastern Pacific with a similar peak just before mid-year and other maxima late in the year. Both figures also show maxima in the western Pacific late in the year.

The agreement is not so good in 1996 when the variance in the model is reduced, compared with 1995, and the variance in the observations is reduced much more. The opposite occurs in 1998, at the end of the El Niño, when both figures show an enhanced variance, but the increase is significantly greater in the observations.

However for the purposes of this paper the key period is during 1997 when the El Niño was developing. Figure 6 shows that as the El Niño developed, the variance dropped almost to zero. In Webb (2018) the corresponding velocity variance plot was taken to indicate reduced mixing, resulting in enhanced transport of the warmest surface water by the NECC.

In Fig. 6 the variance is seen to be reduced in the observations, but it remains much larger than the value calculated from the model data. The changes from 1997 are also much larger in the model than in the observations.

6 Discussion

In a study of the 1982-1983 and 1997-98 El Niños, using data archived from a high resolution global ocean model, Webb (2018) proposed a number of mechanisms which helped trigger both events. The first was the increased strength of the NECC due to a stronger than normal annual Rossby wave. The second was an increase in the temperature of the water advected by the NECC due to reduced mixing of cooler water by tropical instability waves.

Prior to the original paper the realism of the model results had been checked by comparing the model prediction of temperatures in the standard Niño regions with observations. However this study (Webb, 2016) did not investigate the realism of the model SSH values and studied only part of the development in the surface temperature field in space and time.

The present paper has therefore concentrated on aspects of the temperature and SSH field that have most effect on the proposed mechanisms. For the temperature field, the results show that in the Equatorial band, between 1995 and 2000, there

https://doi.org/10.5194/os-2019-86
Preprint. Discussion started: 19 August 2019

Ocean Science
Discussions
Open Access
EGU

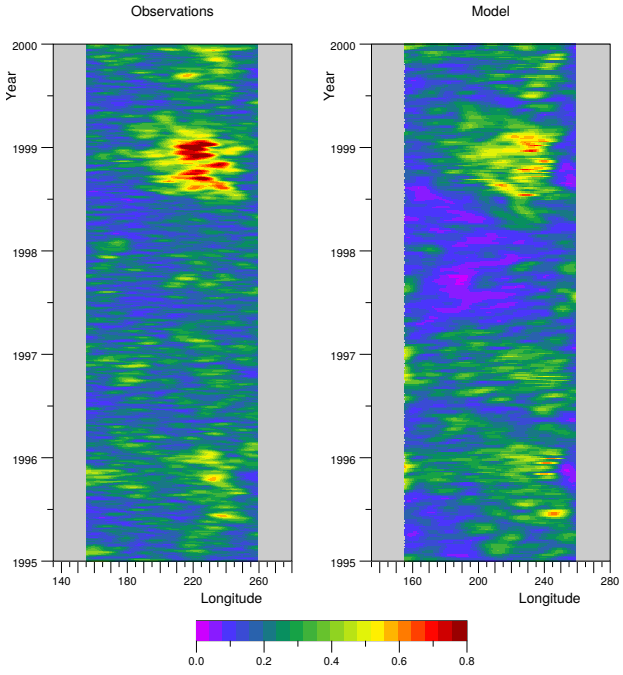

Figure 6. Observed and model sea surface height r.m.s. variance in the Pacific at latitude 6°N between 135°E and 280°E (80°W). Units are meters.

is good agreement between the model and observations. In the autumn of 1997 during the main development phase of the El Niño, there is also good spatial agreement between the model and observations.

The comparison of SSH values at 6°N and at the Equator also show a good agreement. Together with the surface temperature comparison this does not prove the hypothesis about the role of the annual Rossby wave, but it gives no reason to think it is wrong.

In the study of r.m.s. variance, the agreement during the development phase of the El Niño is not so good. During this period, the estimate based on the observed SSH data shows much more variance than that based on the model SSH. This implies that that tropical instability waves were more active in reality than in the model.

However this result is in conflict with the SST observations (Figs. 1 to 3) where temperature fluctuations due to tropical instability waves all but disappeared in the central Pacific. It is thus possible that there is some tropical instability wave activity during a strong El Niño but this is too weak to have a significant effect on the transport of warm water by the NECC.

Alternatively, given the potential errors in the altimeter data referred to earlier, it is possible that the differences in sea level variance during the growth period of the 1997-98 El Niño, results from the noise level of the gridded data.

https://doi.org/10.5194/os-2019-86
Preprint. Discussion started: 19 August 2019

Code and data availability. At the time of publication the model data is freely available at "http://gws-access.ceda.ac.uk/public/nemo/runs/ORCA0083-N06/means/". The Nemo ocean model code and its documentation are available from "http://forge.ipsl.jussieu.fr/nemo/wiki/Users". The satellite temperature data is available from NASA/JPL PODAAC (https://podaac.jpl.nasa.gov/dataset/REYNOLDS_NCEP_L4_SST_OPT_INTERP_WEEKLY_V2). The satellite altimeter data is available from the Copernicus Marine Environment Monitoring Service (ftp://my.cmems-du.eu/Core/SEALEVEL_GLO_PHY_L4 _REP_OBSERVATIONS_008_047/dataset-duacs-rep-global-merged-allsat-phy-l4/).

Competing interests. David Webb is on the advisory board of Ocean Science.

Author contributions. Dr Coward has been involved in developing the NEMO ocean model for many years and was responsible for setting up and running the 1/12°global ocean model and in curating the results. He also provided advice and help in analysing the data. Dr Snaith advised on the selection of satellite data sets, obtained access to the data and is primarily responsible for the discussion of the strengths and weaknesses of the individual datasets. The main author is responsible for the remainder of the paper.

Acknowledgements. This work contributed to and was aided by the research programme of the Marine Systems Modelling group at the UK National Oceanography Centre, part of the Natural Environment Research Council. The Natural Environment Research Council helped fund the investigation through the ODYSEA project (NE/M006107/1) and National Capability funding to NOC. Part of the analysis was carried out using the JASMIN Service at the UK Centre for Environmental Data Analysis, also funded by NERC.

Dr. W. Wimmer provided advice on the satellite datasets. The study depended heavily on the SST data provided by the NASA EOSDIS Physical Oceanography Distributed Active Archive Center at the Jet Propulsion Laboratory, Pasadena, CA (http://dx.doi.org/10.5067/GHGMR-4FJ01) and the SSH data provided by the Copernicus Marine Environment Monitoring Service (https://marine.copernicus.eu).

https://doi.org/10.5194/os-2019-86
Preprint. Discussion started: 19 August 2019

References

Anderson, D. and Rowlands, P.: The role of inertia-gravity and planetary waves in the response of a tropical ocean to the incidence of an equatorial Kelvin wave on a meridional boundary, Journal of Marine Research, 34, 295–312, 1976.

Evans, J. L. and Webster, C. C.: A variable sea surface temperature threshold for tropical convection, Australian meteorological and Oceanographic Journal, 64, S1–S8, https://doi.org/10.22499/2.6401.007, 2014.

Gill, A.: Atmosphere-Ocean Dynamics, Academic Press, 1982.

Kug, J.-S., Jin, F., and An, S.-I.: Two types of El Niño Events: Cold Tongue El Niño and Warm Pool El Niño, Journal of Climate, 22, 1499–1515, https://doi.org/10.1175/2008CLI12624.1, 2009.

McCreary, J.: Eastern tropical ocean response to changing wind systems, in: Review Papers of Equatorial Oceanography - FINE Workshop Proceedings, Nova N.Y.I.T. University Press, Fort Lauderdale, Florida, 1978.

Pujol, M.-I., Faugère, Y., Taburet, G., Dupuy, S., Pelloquin, C., Ablain, M., and Picot, N.: DUCS DT2014: then new multi-mission altimeter data set reprocessed over 20 years, Ocean Science, 12, 1067–2016, https://doi.org/10.5194/os-12-1067-2016, 2016.

Reynolds, R. and Stokes, D.: Reynolds NCEP Level 4 Optimally Interpolated SST Weekly Version 2. Ver. 2. PO.DAAC, CA, USA. Dataset accessed 2019-08-30, https://doi.org/10.5067/REYN2-OIMOW, http://dx.doi.org/10.5067/REYN2-OIMOW, 1981.

Reynolds, R. W., Rayner, N. A., Smith, T. M., Stokes, D. C., and Wang, W.: An improved in situ and satellite SST analysis for climate, Journal of Climate, 15, 1609–1625, 2002.

Taburet, G. and Team, S.-T.: Sea-level-TAC product Quality Information Document, Tech. rep., Copernicus, Ref: CMEMS-SL-QUID-008-032-051, Date: 15 October 2018, Issue: 2.4, http://marine.copernicus.eu/documents/QUID/CMEMS-SL-QUID-008-032-051.pdf.

Webb, D. J.: A comparison of sea surface temperatures in the Equatorial Pacific Nino regions with results from two early runs of the NEMO 1/12° Ocean Model, Research and Consultancy Report, No. 55, National Oceanography Centre, Southampton, U.K., http://nora.nerc.ac.uk/id/eprint/513264, 2016.

Webb, D. J.: On the role of the North Equatorial Current during a strong El Niño, Ocean Science, 14, 633–660, https://doi.org/10.5195/os-14-633-2018, 2018.

Wentz, F. J., Gentlemann, C., Smith, D., and Chelton, D.: Satellite Measurements of Sea Surface Temperature Through Clouds, Science, 288, 847–850, 2000.

Wyrtki, K.: Teleconnections in the Equatorial Pacific Ocean, Science, 180(4081), 66–68, 1973.

Wyrtki, K.: Equatorial Currents in the Pacific 1950 to 1970 and Their Relation to the Trade Winds, Journal of Physical Oceanography, 4, 372–380, 1974.

Wyrtki, K.: El Niño - The Dynamic Response of the Equatorial Pacific Ocean to Atmospheric Forcing, Journal of Physical Oceanography, 5, 372–380, 1975.